

# Contents

<b>Contents</b>	<b>i</b>
<b>List of Figures</b>	<b>ii</b>
<b>List of Tables</b>	<b>iii</b>
<b>1 Ferromagnetism and the Ising Model</b>	<b>1</b>
1.1 Ferromagnetism . . . . .	1
1.2 Ising Model . . . . .	2
1.2.1 Joint Density of States . . . . .	3
1.2.2 Thermodynamics . . . . .	4
1.2.3 Relevance . . . . .	5
<b>2 Monte Carlo Methods Applied to the Ising Model</b>	<b>6</b>
2.1 Metropolis Method . . . . .	6
2.1.1 Success and Limitations . . . . .	7
2.2 Wang-Landau Sampling . . . . .	8
2.2.1 Algorithm . . . . .	8
2.2.2 Success and Limitations . . . . .	9
<b>3 Flat Scan Sampling</b>	<b>10</b>
3.1 Background . . . . .	10
3.2 Algorithm . . . . .	10
3.3 Implementations . . . . .	10
3.3.1 Single Core . . . . .	10
3.3.2 MPI . . . . .	10
3.4 Validation and Convergence . . . . .	10
3.5 Performance . . . . .	10
3.5.1 Amdahl's Law and Parallel Scaling . . . . .	10
3.6 Comparison with Wang-Landau Sampling . . . . .	10
<b>4 Thermodynamics and Finite Size Scaling</b>	<b>11</b>
<b>5 Conclusion and Future Work</b>	<b>12</b>
<b>Bibliography</b>	<b>13</b>

# List of Figures

1.1	(a) Magnetization curve for $\text{La}_{0.67}\text{Ca}_{0.33}\text{MnO}_3$ as a function of temperature;(b) Spins diagram for the ferromagnetic phase (left) and for the paramagnetic phase (right). . . . .	1
1.2	Plot of the exact JDoS for the SS L4 Ising Model with PBC. This was obtained by visiting each microstate available to the system. . . . .	3
2.1	TODO: MORE P VALUES!!!! Mean absolute error of the JDoS for the Ising model computed by the Wang-Landau sampling for a L4 SS lattice plotted against $f_{final} - 1$ . The flatness condition used was 90%. . . . .	9

# List of Tables

- 1.1 Joint Density of States for the SS lattice with  $L = 2$  Ising Model. The rows are the values of energy,  $E$ , and the columns the values of magnetization,  $M$ . 3

# Chapter 1

## Ferromagnetism and the Ising Model

In this Chapter a brief introduction to ferromagnetism is presented, from the history and significance of the Ising model, to the joint density of states and relevant thermodynamic relations and properties obtained from it.

### 1.1 Ferromagnetism

Magnetic materials are critical in our modern society, since they have very broad applications in our daily lives. For example, there are magnetic materials in every speaker and microphone, hard-drive disks on our computers, they play a big role in medicine where they are used in body scanners (usually in MRI machines) and together with applications in electric motors, transformers and generators [1]. Magnetic materials can be classified in terms of their magnetic properties, such as diamagnetism, paramagnetism, ferromagnetism, and so forth [2].

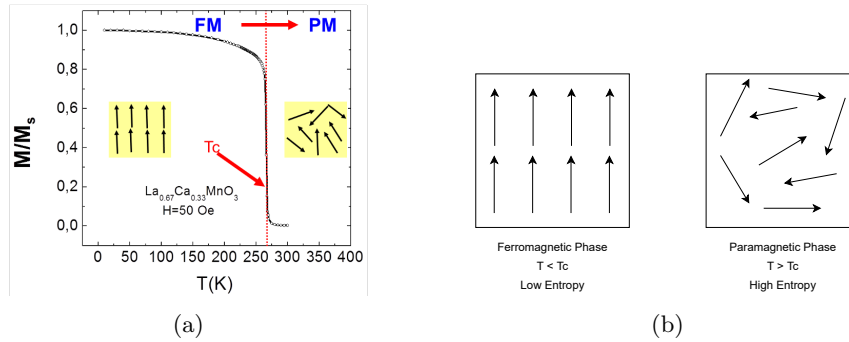


Figure 1.1: (a) Magnetization curve for  $\text{La}_{0.67}\text{Ca}_{0.33}\text{MnO}_3$  as a function of temperature; (b) Spins diagram for the ferromagnetic phase (left) and for the paramagnetic phase (right).

A ferromagnetic material exhibits spontaneous magnetization in the absence of an applied external magnetic field. This way, the magnetic moments of the atoms that compose the material are all naturally aligned along one direction [3]. One of the key features of ferromagnetic materials is that they only display this property below a certain well-defined critical temperature,  $T_C$ , usually called the Curie temperature. This temperature defines a phase transition between a ferromagnetic and a paramagnetic state, figure 1.1(a). Above the Curie temperature, the entropy within the material becomes too strong and the magnetic

moments start to dis-align, thus the materials loses its spontaneous magnetization, figure 1.1(b). In other words, the effect due to thermal disorder overtakes the ferromagnetic order.

This kind of nature is common to various transition metal, Iron, Cobalt, Nickel, and so forth, and to some rare earth materials, such as Gadolinium. One application of ferromagnets is magnetic refrigeration. This is based on the magnetocaloric effect (MCE), which consists of a change in temperature of a magnetic material by the application and removal of an external magnetic field., known as the magnetocaloric effect (MCE). For a ferromagnetic material, the MCE is more prominent when the magnetic field is applied for temperatures around the Curie temperature. High performance magnetic refrigerants include the LaFeSi 1:13 family [4] and MnFeP based intermetallics [5].

In the recent years, computational materials design is becoming the new norm to discover new materials by combining computer science with quantum and statistical mechanics. It is more advantageous than the experimental sciences since it is not as time-consuming and bounded by high costs in equipment as running an experiment [6, 7, 8].

## 1.2 Ising Model

In 1920 Wilhelm Lenz, a German physicist, gave Ernest Ising, his PhD student, an exercise that considered a one-dimensional chain of spin-1/2 particles that can be either pointing up or down. The spins can only interact with their neighbours. Later in 1925, Ising solved this problem, awarding him a doctorate in physics, and concluded that there was no phase transition in the one-dimensional case and wrongly extrapolated that there was no phase transition in higher dimensions [9].

It was not until 1944 that a Norwegian-born American physicist, Lars Onsager, solved the much harder two-dimensional case analytically, in a square lattice [10]. In this case, Onsager showed that there is a well defined phase transition from a ferromagnetic to a paramagnetic state at a critical temperature ( $T_C$ ), therefore proving Ising's extrapolation wrong.

Since then, the Ising Model has become one of the most studied and published physical models, since it has a non-trivial phase transition while being able to have an analytical solution, at least for dimensions lower or equal to two. As of yet, there are no exact solutions for higher dimensions. We are only able to get properties from three dimensional lattices by numerical simulation.

The Ising Hamiltonian describes a system of lattice of atomic spins which can have two spin directions, up (+1) and down (-1) with neighbour to neighbour interactions. So, it is written as

$$\mathcal{H} = - \sum_{\langle i,j \rangle} J_{ij} \mathbf{S}_i \cdot \mathbf{S}_j - H \sum_i \mathbf{S}_i \quad (1.1)$$

where  $J$  is the interaction for constant between two neighbouring particles,  $S_i$  is the spin value of the particle at the site  $i$ ,  $\langle i, j \rangle$  denotes that the sum is conducted over all neighbouring particles. The second term represents the interaction with an external magnetic field,  $H$ , and it is completely optional. If  $J > 0$ , the system will have a ferromagnetic behaviour since parallel spins are energetically more favourable, and if  $J < 0$ , the system will behave in an anti-ferromagnetic way.

In this work, I will not evaluate the Ising Model with an applied magnetic field,  $H = 0$ , and consider  $J_{ij} = 1$  to simplify the computations. With this being said, the Hamiltonian treated in this work goes as follows,

$$\mathcal{H} = - \sum_{\langle i,j \rangle} \mathbf{S}_i \cdot \mathbf{S}_j \equiv -\frac{1}{2} \sum_{ij} \mathbf{S}_i \cdot \mathbf{S}_j \quad (1.2)$$

To simulate real materials we can obtain the values of the interaction constant for each atom in our lattice through Density Functional Theory (DFT) calculations [11].

### 1.2.1 Joint Density of States

It is mentioned in any undergraduate course in statistical mechanics that the density of states (DoS),  $g(E)dE$ , gives the number of states that have a certain energy between  $E$  and  $E + dE$  [12]. For discrete systems, like the Ising Model, the DoS evaluated at a certain energy gives us the exact number of microstates that have a specific energy  $E$ . Through the DoS we can obtain the partition function  $Z(T)$ , as a function of temperature, and then compute energy related thermodynamic variables, such as the mean energy  $E(T)$ , specific heat  $C(T)$ , Helmholtz free energy,  $F(T)$ .

As we are dealing with magnetic systems our natural interest is to study the magnetization throughout various temperatures and applied magnetic field intensity. For this, we need the number of microstates with a certain pair  $(E, M)$ . This is the exact description of the Joint Density of States (JDoS), a multi-variable histogram with information about the number of microstates with a certain energy and another parameter, like density,  $\rho$ , number of particles,  $N$ , or, in this case, magnetization,  $M$ . This way we can compute the partition function as a function of both temperature and magnetization,  $Z(T, M)$  and the Helmholtz free energy as  $F(T, M)$ .

Table 1.1 represents the JDoS for the Ising Model in a simple square (SS) lattice with length 2 and periodic boundary conditions (PBC). The extreme magnetization configurations appear only once in the JDoS, no matter the size of the lattice, since they represent all up or all down spins configurations.

Table 1.1: Joint Density of States for the SS lattice with  $L = 2$  Ising Model. The rows are the values of energy,  $E$ , and the columns the values of magnetization,  $M$ .

$E / M$	-4	-2	0	+2	+4
-8	1	0	0	0	1
-4	0	0	0	0	0
0	0	4	4	4	0
+4	0	0	0	0	0
+8	0	0	2	0	0

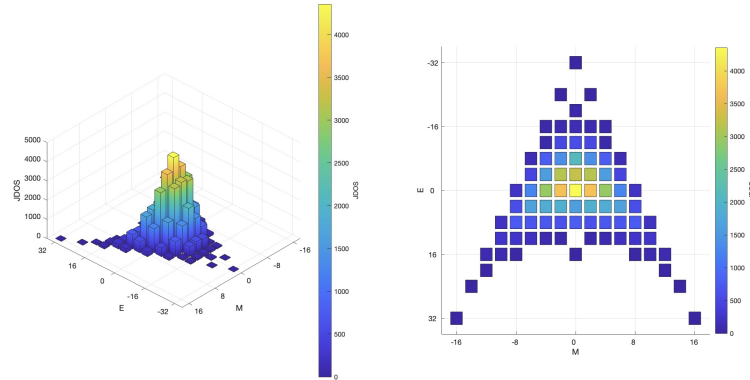


Figure 1.2: Plot of the exact JDoS for the SS L4 Ising Model with PBC. This was obtained by visiting each microstate available to the system.

There are three configurations worth noting. The first is the zero energy and zero magnetization state. This is the state with the most micro configurations since it represents the macrostate in which is likely to find the system in, when  $T \gg T_C$  (has the highest entropy). The second is the macrostate with the highest energy and zero magnetization. For every system size and lattice this macrostate has always 2 microstates, since the spins are sorted in a chess/checker board pattern. The last configuration is the macrostate with the least energy and zero magnetization. Its value is always going to be equal to  $2L$ , since the spins are sorted in rows and columns of alternating positive and negative spins, similar to slices. Throughout this work these configurations will appear again and they will be called, ZeroZero, Checker Board and Slice, respectively.

To compute the JDoS it is necessary to visit all of the possible microstates. It is easy to do this until we have 16 spins ( $L = 4$  in a SS lattice, figure 1.2), since the number of possible configurations is still quite small,  $Q = 2^{16} \sim 65E3$ . But, for instance, for systems with 256 spins ( $L = 8$  in a SS lattice) it becomes computationally impossible to randomly or sequentially visit all of the microstates since we have to sample  $Q = 2^{256} \sim 1E77$  configurations. Instead we can use various clever numerical methods to get an estimation of the JDoS in a much more reasonable time with fairly good precision. I will present widely studied methods in the next Chapter and a new unpublished method in the third Chapter.

### 1.2.2 Thermodynamics

From the JDoS we can obtain all of the thermodynamic quantities when the system is in an equilibrium state. In this section I will present some useful formulas to compute those variables from the JDoS. The probability of a given state with energy  $E_i$ , is given by

$$P(E_i) = \frac{\sum_q g(E_i, M_q) \exp(-\beta E_i)}{Z}, \quad (1.3)$$

where  $\beta$  is defined as  $\beta \equiv 1/k_B T$  and  $Z$  is the canonical partition function given by

$$Z = \sum_q Z(T, M_q) = \sum_q \sum_i g(E_i, M_q) \exp(-\beta E_i). \quad (1.4)$$

From this we can obtain mean thermodynamic variables,

$$\langle E \rangle = \frac{1}{Z} \sum_i \sum_q E_i g(E_i, M_q) \exp(-\beta E_i), \quad (1.5)$$

$$\langle M \rangle = \frac{1}{Z} \sum_q \sum_i M_q g(E_i, M_q) \exp(-\beta E_i) \equiv \frac{1}{Z} \sum_q M_q Z(T, M_q). \quad (1.6)$$

$\langle E \rangle$  is related to the specific heat by

$$\langle C \rangle = \frac{\langle E^2 \rangle - \langle E \rangle^2}{(k_B T)^2}, \quad (1.7)$$

then to obtain the mean entropy we use the second law of thermodynamics,

$$\langle S \rangle = \int \frac{\langle C \rangle}{T} dT. \quad (1.8)$$

However there is another way to estimate thermodynamic properties, from the estimated JDoS. Using the Helmholtz free energy, defined as

$$F(T, M) = -k_B \ln(Z(T, M)) \quad (1.9)$$

and the principle of minimum energy, we can extract  $F_{min}(T) = \min(F(M, T))$ , which is defined as the lowest temperature-dependent free energy that can be reached by the system. From it we can obtain the magnetization and energy for that value of free energy minima,  $M_{F_{min}}$  and  $E_{F_{min}}$ , respectively. Through  $F_{min}$  we can use the following thermodynamic relations to compute the specific heat and entropy of the system:

$$C = -T \frac{\partial^2 F_{min}}{\partial T^2}, \quad (1.10)$$

$$S = -\frac{\partial F_{min}}{\partial T}. \quad (1.11)$$

### 1.2.3 Relevance

Despite its simplicity and age, the Ising Model is used in a multitude of research fields within the physical sciences and the social sciences.

Within the physical sciences the Ising Model is used to simulate not only magnetic materials but also systems that are characterized by nearest-neighbour interactions and undergo a phase transition Ising-like, this means systems that go from an ordered-low entropy phase to a disordered-high entropy phase at a specific critical temperature [13]. Liquid vapour transitions, where the order parameter is the density,  $\rho$ , binary liquid mixtures, where the order parameter is the concentration and the transition corresponds to the mixing of the two liquids.

In the social sciences, the Ising Model has been used to describe a plethora of theoretical models of social behaviour and model financial markets [14]. Topics ranging from the study of racial segregation in certain communities [15], to a demonstration that a community that speaks only one language can start speaking another one without any outside bias [16].

In economics Monte Carlo methods are widely used to model financial markets due to its randomness, and the Ising Model is the standard model that those methods are applied to. In these case studies the spins are the option of buying or selling a certain stock through neighbour to neighbour communication or external factors. The magnetization represents the average actions of the stock market agents [17, 18].



## Chapter 2

# Monte Carlo Methods Applied to the Ising Model

A short review of the Monte Carlo (MC) methods used to solve the Ising Model in the current paradigm is presented. There will be a focus on the famous Metropolis Method and the Wang-Landau sampling.

### 2.1 Metropolis Method

The classic Metropolis method, introduced in 1953 by Metropolis et al., belongs to the Markov chain Monte Carlo (MCMC) class of algorithms. These algorithms exploit the fact that if we construct a Markov chain that has a specific equilibrium distribution one can obtain samples recording the states generated by the Markov chain.

In a brief fashion, a Markov chain is a stochastic model that describes a sequence of possible events, in this case microstates, in which the probability of transiting to another state depends on the current state. This way the probability of the next state,  $S_j$ , given the current state,  $S_i$ , can be written as

$$P(S_j, t) = \sum_i W(S_i \rightarrow S_j) P(S_i, t), \quad (2.1)$$

where  $W(S_i \rightarrow S_j) \equiv W_{ij}$  is the transition probability to move from the state  $i$  to  $j$ . We require that

$$W_{ij} \geq 0 \quad \sum_j W_{ij} = 1. \quad (2.2)$$

The master equation considers the change of the probability of the next state with time,  $t$ ,

$$\frac{dP(S_j, t)}{dt} = \sum_i [W_{ij} P(S_i, t) - W_{ji} P(S_j, t)]. \quad (2.3)$$

In the equilibrium regime, the master equation has to equal 0, and we get the detailed balance condition for the equilibrium probability  $P_{eq}(S_j)$ ,

$$W_{ji} P_{eq}(S_j) = W_{ij} P_{eq}(S_i). \quad (2.4)$$

The object of Metropolis Sampling is to generate canonical configurations with an equilibrium probability

$$P_{eq}(E_i) = \frac{\exp(-\beta E_i)}{Z}. \quad (2.5)$$

Here  $Z$  is the partition function, however this is usually not known before hand. When considering a Markovian process we generate each new configuration from the preceding one avoiding this problem. As a result the difference of energy between the two states is needed,  $\Delta E = E_i - E_j$  and the transition probability of given as

$$W_{ij} = \begin{cases} \tau_0^{-1} \exp(-\beta \Delta E) & \text{if } \Delta E \geq 0 \\ \tau_0^{-1} & \text{if } \Delta E < 0 \end{cases} \quad (2.6)$$

where  $\tau_0^{-1}$  is the time required to attempt a spin-flip. We often set this time unit to one.

This way the Metropolis method applied to the Ising Model, with a fixed external magnetic field and a fixed temperature, goes as follows:

1. Choose an initial state;
2. Choose a spin  $i$  and perform a spin-flip;
3. Calculate the energy change from that spin-flip,  $\Delta E$ ;
4. Accept the flip with a probability  $\min(1, \exp(-\beta \Delta E))$ ;
5. When the system reaches equilibrium, measure any thermodynamic quantity needed;
6. Go back to (2) and repeat until there is enough samples of the thermodynamic variables.

Note that we accept the spin flip if a given uniformly random number  $r, r \in [0, 1]$ , is less or equal to the acceptance criteria. Typically in Monte Carlo simulations we define the MC time as the amount of trial flips equal to the number of spins in our lattice,  $N$ .

### 2.1.1 Success and Limitations

The Metropolis sampling proposed by Metropolis et al., can be successfully applied to an array of models, ranging from widely studied quantum ensembles and gases simulations to state-of-the-art protein and peptide simulations and to machine learning and neural networks. The following paragraphs will be directed to magnetic systems, like the Ising model, but they can be extrapolated to others physical systems.

When getting thermodynamic variables we have to let the simulation reach the equilibrium stage, where the probability distribution takes the form of equation 2.5. Then we take a measurement each MC time, resulting in  $M$  total values for that variable. At the end the average of that variable,  $A$ , is taken  $\langle A \rangle = \frac{1}{M} \sum_i A_i$ . For large systems the time taken to reach equilibrium stage is often very long thus making the simulation time consuming. This is worsened by the fact that to study how some thermodynamic variable  $A$  changes over a wide range of temperatures or applied fields intensities, we need to run multiple Metropolis simulations for each temperature and field intensity values, making this process very time-consuming.

Lastly there is another shortcoming known as critical slowing down. In short, for computations where the temperature is near the critical temperature,  $T_C$ , the sampling slows down, meaning that it is more time-consuming for the computations to reach the equilibrium stage, thus slowing down the overall simulation.

## 2.2 Wang-Landau Sampling

Since its introduction the Metropolis sampling was the go-to method to study phase transitions and critical phenomena in condensed matter physics and statistical mechanics. In the final decades of the 20th century scientists were committed to develop new methods that could overcome the shortcomings of the Metropolis Sampling. Various methods were proposed such as the cluster flip algorithms, where Swendsen and Wang were pioneers, and the multicanonical ensemble method. The first solved the critical slowing down present in the Metropolis and the second could sample rough energy landscapes with ease.

In 2001, Fugao Wang and David P. Landau proposed a new Monte Carlo method, now called the Wang-Landau method or sampling. The goal of this method diverges from the goal of previous methods. Instead of generating configurations with a canonical probability, this method tries to estimate the canonical partition function

$$Z = \sum_E g(E) \exp(-\beta E) \quad (2.7)$$

through the estimation of the density of states  $g(E)$  from a flat histogram in the phase space.

The main difficulty of a simple random walk in the energy space is that the walker would spend most of its time in the highest probable states thus making the random walk ineffective. The idea of the Wang-Landau sampling is to do a random walk, Metropolis like, and accepting the new states with a probability proportional to the inverse to their DoS  $\frac{1}{g(E)}$ . Doing this we obtain a flat histogram meaning that each macrostate has the same probability of being visited. Since  $g(E)$  is unknown *a priori*, in each step of the random walk,  $g(E)$  is also being constructed.

The algorithm was proposed to compute the DoS but, it can also estimate the JDoS by performing the random walk in the phase space composed by energy,  $E$ , and the second order parameter, in our case, the magnetization of the system,  $M$ . This comes with a downside, since the JDoS has 1000x more information than the DoS it takes 1000x more time to compute.

### 2.2.1 Algorithm

First we start with an arbitrary configuration of spins and a guess for the density of states. Usually, this guess is  $g(E, M) = 1$ . Choosing a random site in our lattice, we perform a trial flip and compute the energy-magnetization pair before the trial,  $(E_i, M_i)$ , and after,  $(E_j, M_j)$ . The new configuration is accepted with a probability

$$P((E_i, M_i) \rightarrow (E_j, M_j)) = \min \left( 1, \frac{g(E_i, M_i)}{g(E_j, M_j)} \right). \quad (2.8)$$

Whether the configuration is accepted or rejected, we have to update the histogram and refine the DoS estimation. This way, being the system in the state  $(E, M)$ ,

$$H(E, M) = H(E, M) + 1,$$

and we multiply the current value of the DoS by a modification factor,  $f > 1$ ,

$$g(E, M) = f g(E, M).$$

A reasonable choice for the initial value of the modification factor is  $f_0 = e$ . If  $f_0$  is too small, the simulation will take a very long time to reach all of the possible macrostates,  $(E, M)$ . If it is too large, then we will have large statistical errors. This process is repeated until the

histogram is considered "flat", all of the possible energies have been visited the same number of times. As it is impossible to obtain a 100% flat histogram, we define a rule for flatness as  $\min(H(E, M)) > \langle H(E, M) \rangle \times p$ ;  $p$  is chosen according to the size of the problem. For small cases, such as the two dimensional Ising model,  $p$  can be set as high as 0.95, but for larger systems the flatness condition may never be satisfied if  $p$  is near unity. Once a flat histogram is reached, we set  $H(E, M) = 0$ , keep the estimation of the DoS and reduce the modification factor,  $\sqrt{f_i} \rightarrow f_{i+1}$  and continue the random walk. We stop the simulation if  $f < f_{final}$ , where  $f_{final}$  is a number very close to one (often  $f_{final} \sim 1 + 1/E - 8$ ).

At the end, the method gives us the relative density of states. To determine the normalized DoS we can use the fact that

$$\sum_{E, M} g(E, M) = 2^N. \quad (2.9)$$

### 2.2.2 Success and Limitations

The modification factor controls the accuracy and the steps taken to reach a flat histogram in our computations. As it approaches unity, the number of iterations goes to infinity. This way, at the beginning of the simulation, when the modification factor is large, the estimation of the DoS is quite bad, since there we are taking fewer samples with a high weight. At the later stages, the modification factor is lower therefore we have more samples of each macrostate with a lower overall weight. This way, the initial stages of the simulation are characterized by the accumulation of low precision statistics and the later stages by the refining of the firsts samples.

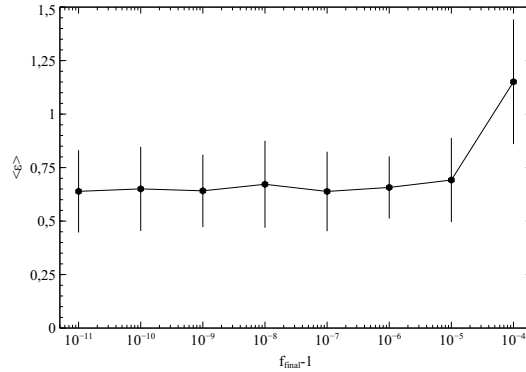


Figure 2.1: TODO: MORE P VALUES!!!! Mean absolute error of the JDoS for the Ising model computed by the Wang-Landau sampling for a L4 SS lattice plotted against  $f_{final} - 1$ . The flatness condition used was 90%.

Due to the wrong samples at the initial stages of the computations, the final estimation of the JDoS will never converge to the exact solution. In the figure 2.1 we can see that the absolute value of the mean error never converges to zero, thus the method has an intrinsic source of error.

## Chapter 3

# Flat Scan Sampling

### 3.1 Background

### 3.2 Algorithm

### 3.3 Implementations

#### 3.3.1 Single Core

#### 3.3.2 MPI

### 3.4 Validation and Convergence

### 3.5 Performance

#### 3.5.1 Amdahl's Law and Parallel Scaling

### 3.6 Comparison with Wang-Landau Sampling

## Chapter 4

# Thermodynamics and Finite Size Scaling

## Chapter 5

# Conclusion and Future Work

# Bibliography

- [1] O. Gutfleisch, M. A. Willard, E. Brück, C. H. Chen, S. G. Sankar, and J. P. Liu, “Magnetic materials and devices for the 21st century: Stronger, lighter, and more energy efficient,” *Advanced Materials*, vol. 23, no. 7, pp. 821–842, 2011.
- [2] D. J. Griffiths, *Introduction to Electrodynamics*. Cambridge University Press, 4th ed., 2013.
- [3] Stephen Blundell, *Magnetism in Condensed Matter*. 2001.
- [4] A. Fujita, S. Fujieda, Y. Hasegawa, and K. Fukamichi, “Itinerant-electron metamagnetic transition and large magnetocaloric effects in  $\text{La}(\text{Fe}_{1-x}\text{Si}_x)_3$  compounds and their hydrides,” *Physical Review B - Condensed Matter and Materials Physics*, vol. 67, no. 10, pp. 1044161–10441612, 2003.
- [5] O. Tegus, E. Brueck, K. H. J. Buschow, and F. R. de Boer, “Transition-Metal-Based Magnetic Refrigerants for Room-Temperature Applications,” *ChemInform*, vol. 33, no. 14, pp. no–no, 2010.
- [6] S. Curtarolo, G. L. Hart, M. B. Nardelli, N. Mingo, S. Sanvito, and O. Levy, “The high-throughput highway to computational materials design,” *Nature Materials*, vol. 12, no. 3, pp. 191–201, 2013.
- [7] W. Chen, J. George, J. B. Varley, G. M. Rignanese, and G. Hautier, “High-throughput computational discovery of  $\text{In}_2\text{Mn}_2\text{O}_7$  as a high Curie temperature ferromagnetic semiconductor for spintronics,” *npj Computational Materials*, vol. 5, no. 1, 2019.
- [8] S. Sanvito, C. Oses, J. Xue, A. Tiwari, M. Zic, T. Archer, P. Tozcan, M. Venkatesan, M. Coey, and S. Curtarolo, “Accelerated discovery of new magnets in the Heusler alloy family,” *Science Advances*, vol. 3, no. 4, pp. 1–10, 2017.
- [9] E. Ising, “Beitrag zur Theorie des Ferromagnetismus,” *Zeitschrift für Physik*, vol. 31, no. 1, pp. 253–258, 1925.
- [10] L. Onsager, “A Two-Dimensional Model with an Order-Disorder Transition,” *Physical Review Letters*, vol. 65, no. 3 and 4, pp. 117–149, 1944.
- [11] G. Bihlmayer, *Density Functional Theory for Magnetism and Magnetic Anisotropy*. 2020.
- [12] R. K. Pathria and P. D. Beale, *Statistical Mechanics*. 3rd ed.
- [13] A. Pelissetto and E. Vicari, “Critical phenomena and renormalization-group theory,” *Physics Report*, vol. 368, no. 6, pp. 549–727, 2002.
- [14] D. Stauffer, “Social applications of two-dimensional Ising models,” *American Journal of Physics*, vol. 76, no. 4, pp. 470–473, 2008.



- 
- [15] P. Abell and P. Abell, “The Journal of Mathematical Sociology Some Aspects of Narrative Method,” no. July 2015, pp. 37–41, 2010.
  - [16] D. Nettle, “Is the rate of linguistic change constant?,” *Lingua*, vol. 108, no. 2-3, pp. 119–136, 1999.
  - [17] L. Damodaran and K. M. Udayanandan, “Dynamics of stock market , using Ising model,” pp. 71–78.
  - [18] P. dvorak, “Ising Model in Finance From Microscopic Rules to Macroscopic Phenomena,” pp. 1–56, 2012.